PICTURE OF THE MONTH

Cloud Radar Observations of Kelvin–Helmholtz Instability in a Florida Anvil

JACOB M. PETRE AND JOHANNES VERLINDE

Department of Meteorology, The Pennsylvania State University, University Park, Pennsylvania

8 January 2004 and 23 April 2004

1. Introduction

Tropical anvils are frequently considered to be well-mixed layers (Lilly 1988), with radiative cooling at cloud top providing the mixing mechanism (Ackerman et al. 1988). Contrary to this assumption, after dusk on 21 July 2002, a vertically pointing radar at the Kendall-Tamiami Airport in Miami, Florida, detected persistent shear instability, also known as Kelvin–Helmholtz instability, in a convective outflow anvil. To our knowledge, the observations presented in this paper are the first documented large-amplitude, embedded Kelvin–Helmholtz billows inside a tropical anvil and point to a distinct layering in the anvil.

Radar has been used before to detect shear instability in the atmosphere. The early work of Gossard and Richter (1970) and Gossard et al. (1971) described the detailed structures of shear instability in clear air using a vertically pointing, frequency-modulated, continuous-wave radar system operating at a wavelength of 100 mm. Browning (1971) conducted radar observations of shear instability in the United Kingdom and documented numerous episodes, mostly in clear-air turbulence near the jet stream. This phenomenon also occurs in clouds; for example, Weckworth and Wakimoto (1992), Martner and Ralph (1993), and Chapman and Browning (1997) captured radar imagery of Kelvin–Helmholtz billows in clouds associated with strong shear situations. In either case, a distinct interlaced double-sinusoidal structure first described by Kelvin (1880) characterizes this type of instability and allows for easy identification.

2. Data and methods

The cloud radar data presented in this paper were collected by the University of Miami Radar Laboratory Group at the Kendall-Tamiami Executive Airport in Miami on 21–22 July 2002 as part of the Cirrus Regional Study of Tropical Anvils and Cirrus Layers–Florida Area Cirrus Experiment (CRYSTAL–FACE). The University of Miami 95-GHz radar is described in detail by Lhermitte (1987). The data collection occurred between 0100 and 0500 UTC on 22 July 2002, or 2100 to 0100 eastern daylight time (EDT; local time) 21–22 July 2002. The life cycle of an anvil was sampled from shortly after its initiation by convection through its detached anvil stage; afterward, the anvil advected eastward, away from the radar site, while the radar sampled the trailing anvil.

The radar system recorded calibrated in-phase and quadrature values from every pulse and range gate from the surface to an altitude of 15 210 m with a vertical resolution of 30 m. Such high spatial resolution, combined with the excellent sensitivity to small scatterers, enable the radar to reveal small and subtle features within clouds. These basic measurements were processed to provide velocity power spectra for every range gate every 2 to 3 s (Kollias et al. 2001). Because most spectra exhibited a sharp drop-off in power at their slow-falling edges—indicative of low turbulence conditions—the volume-mean air velocity was taken as the velocity of the slowest-falling particles with signal above the noise (Babb et al. 1999; estimated error $< \pm 0.1$ m s^{-1}). In addition to the volume-mean air velocity, the total reflectivity and Doppler spread were calculated.

3. Results and discussion

Figure 1 presents time–height evolutions of the radar reflectivity, the volume-mean air velocity, and the Doppler spread. The left-hand side of each image represents the time when convection was still active close to the radar, and the right-hand side represents the detached anvil. The reflectivity image (Fig. 1a) reveals a descending pattern throughout the period, associated mostly with precipitation, leaving smaller, low-reflectivity particles at cloud top. The radar-resolved cloud-top region

Corresponding author address: Hans Verlinde, Dept. of Meteorology, The Pennsylvania State University, University Park, PA 16802.
E-mail: verlinde@ems.psu.edu

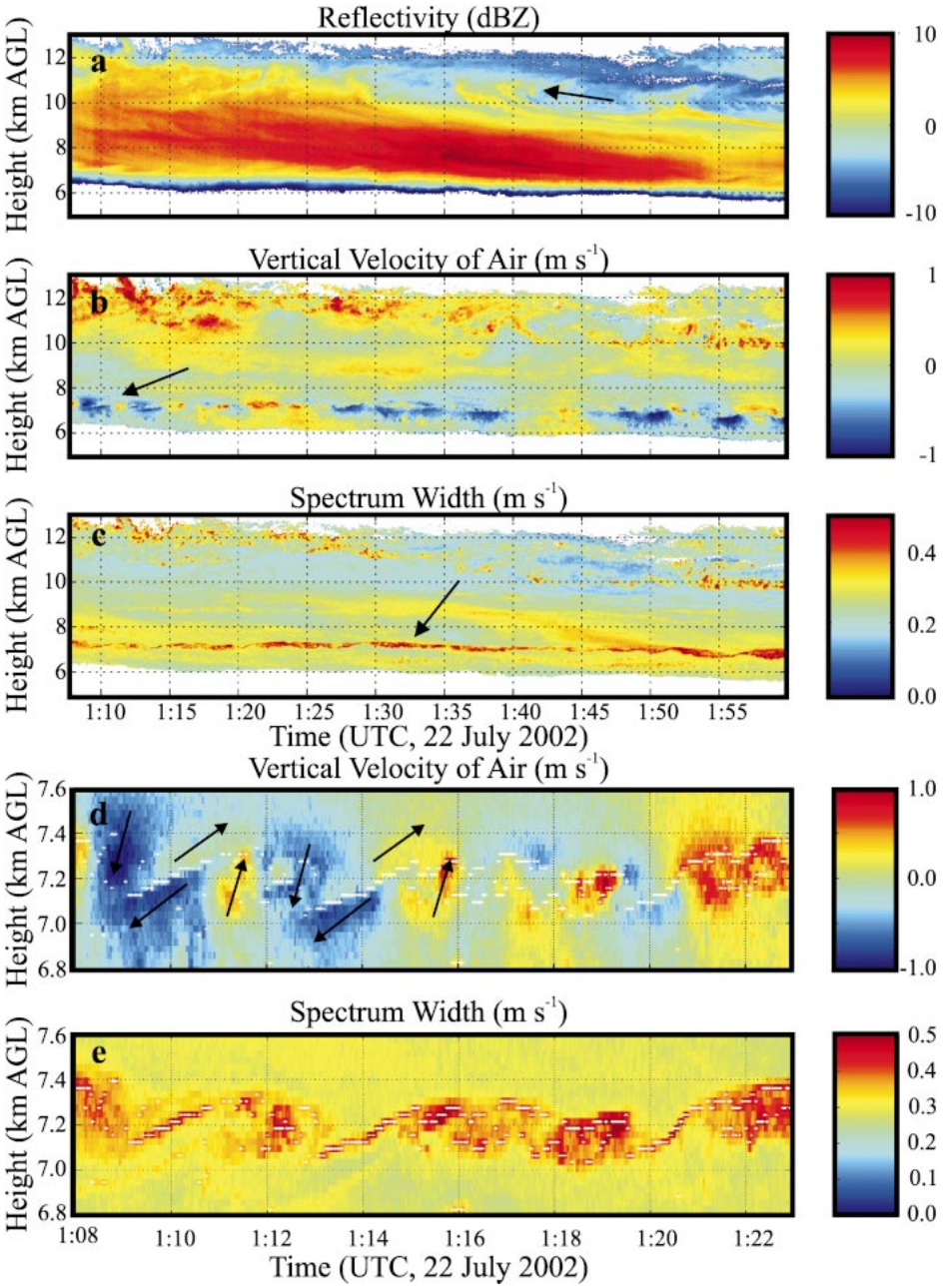

FIG. 1. Radar reflectivity (dBZ), vertical velocity of the air (m s^{-1}), and Doppler spread (m s^{-1}) in the anvil from the University of Miami vertically pointing cloud radar. The arrows point to (a) an embedded generating cell, and (b),(c) a long-lasting shear line. (d),(e) High-resolution views of the vertical velocity of the air (m s^{-1}) and Doppler spread (m s^{-1}) fields of the well-developed shear instability. The white dots track the axis of the maximum Doppler spread.

exhibits mostly upward air motion (Fig. 1b), varying between 0 and 1 m s^{-1} over brief periods, indicative of generating cells. The method used to determine the air motion likely results in an overestimation of the velocity in this turbulent region (Giangrande et al. 2001). As the anvil matures, these generating cells gradually sink deeper into the anvil, eventually becoming deeply embedded in the anvil (indicated by the arrows, more than 2 km below cloud top). The lower part of the anvil exhibits predominantly descending motion, consistent with expectations for anvil regions on mesoscale convective complexes.

The most notable feature in these images can be seen in the velocity and Doppler spread fields at 7 km, while several other similar though less conspicuous features can be found in the velocity and Doppler spread fields

(e.g., at 9 km early in the period). An understanding of the causes of high spread in profiling Doppler spectra is critical for the interpretation of these features.

Wide spectra can be produced by either 1) hydrometeors within the radar volume with wide-ranging fall velocities, or 2) sub-radar-volume velocity fluctuations. An example of the first can be seen at the high Doppler spread associated with the embedded generating cell. The fall streak emanating from the generating cell represents a region where precipitating hydrometeors fall through the population of otherwise smaller hydrometeors, producing a wide Doppler spread.

A closer view of the features in the velocity and Doppler spread fields at 7 km (Figs. 1d,e) reveal a clearly different pattern. Here the Doppler spread feature is frequently only a single range gate (30 m) wide and is situated in an almost uniform reflectivity field. Velocity fluctuations within the radar volume, therefore, must produce the high Doppler spread. At times (Fig. 1e, 0110 UTC, 0114 UTC), this turbulence is confined to a layer less than 30 m in depth, the narrowness of which suggests that the velocity fluctuations result from turbulence generated by vertical shear of the horizontal wind confined to a very narrow layer. At other times, however, the sharply defined line broadens into a diffuse, turbulent structure through the entire 300-m depth of the feature.

To highlight better the structure of the shear layer, we added white markers on both the volume-mean air vertical velocity and Doppler spread images in Figs. 1d,e. These markers represent local maxima of the Doppler spread fields in each profile; they serve to indicate the axis of maximum shear or ''boundary'' between the two cloud layers on the velocity plot. Each of these points satisfies a set of objective criteria applied to its respective vertical profile: all spectra within 100-m vertical separation of the point 1) must have sufficient signal to process; 2) must be primary maximum, defined as having no higher Doppler spread within 100 m; and 3) must exceed the minimum Doppler spread within 100 m by at least 0.0652 m s^{-1}. Taken as a whole, the structure of this shear layer resembles a breaking wave with interlaced sinusoids, reminiscent of Kelvin's (1880) ''cat's eye'' vortices, long associated with shear instability (see further, Browning 1971; Reiss and Corona 1977).

To further illustrate the resemblance to Kelvin–Helmholtz billows, arrows of the relative air motion, deduced from the vertical velocity pattern, have been drawn on the velocity image (Fig. 1d). These velocity vectors generally support a hypothesis that the air in the lower layer below the shear axis moves (relatively) to the left while the air in the upper layer moves to the right. Kelvin–Helmholtz instability occurs when two layers of different densities experience a relative shear across the density interface. The deduced flow field, with shear across the Doppler spread maximum, is consistent with that expected in developing shear instability. We then conclude that these observed features in the velocity and Doppler spread fields indicate shear instability in the interior of the anvil. This shear instability occurs within the cloud; lidar observations confirmed that the visible cloud base was at approximately 6 km, 1 km below the shear instability.

Theory suggests that the instability occurs when the layer gradient Richardson number $\mathrm{Ri}(\Delta Z) = (g/\theta)(\Delta\theta/\Delta Z)/(\Delta V/\Delta Z)^2$ drops below a critical value. Although no sounding passed through these particular anvils during the measurement period, the National Weather Service office in Miami released a balloon-based radiosonde that penetrated another anvil about an hour and a half before these radar observations. The anvil penetrated by this sounding extended from cloud base, just above 7 km, to a cloud top well above 11 km. Computation using centered differences reveals no Richardson number less than 0.25, the presumed critical value. The critical Richardson number, however, depends significantly on the resolution of the measurements used to calculate it. In his half-year study of Kelvin–Helmholtz billows in the United Kingdom, Browning (1971) observed five events with Richardson numbers greater than 0.5 based upon hourly radiosonde data with a 400-m vertical resolution. Using the criterion that $\mathrm{Ri} < 2$ indicates possible conditions for shear instability, the National Weather Service sounding shows that conditions conducive to shear instability may have existed at altitudes of 7.1 km ($\mathrm{Ri} = 0.32$), 7.4 km ($\mathrm{Ri} = 1.8$), and 9.7 km ($\mathrm{Ri} = 1.7$).

The shear instability at 7 km lasted for the full hour presented here; observations not presented show that it lasted for an additional 2.5 h, slowly descending about 1 km to the cloud base. When the shear instability reached cloud base, the radar operators made visual observations of mammatus (Jo et al. 2003). Martner (1995) hypothesizes that the mamma clouds that he observed west of Thompson, Manitoba, Canada, formed from a Kelvin–Helmholtz billow or another wave phenomenon within the interior of the cloud.

In his long-term study of Kelvin–Helmholtz billows in the United Kingdom Browning (1971) noted 16 shear-instability events. A quarter of these appeared for less than 2 min; half of the events lasted 10 min or less, and only one endured more than 18 min. This long-duration event of Browning (1971) lasted more than 4 h, occurring near the tropopause along the axis of the jet stream as clear-air turbulence. Another long-lasting event of Kelvin–Helmholtz billows was described by Chapman and Browning (1997). In this case, the billows were associated with a warm front approaching the southwestern United Kingdom and persisted for 3 h near the surface.

The vertical mixing associated with Kelvin–Helmholtz instability tends to weaken the shear that defines this phenomenon sufficiently to cause its demise; therefore, hours-long episodes of Kelvin–Helmholtz billows require a continuous shear-generating mechanism, such

as a frontal boundary. With a vertical mixing depth of 300 m and a maximum vertical speed of 1 m s^{-1} (Fig. 1d), the eddy associated with the shear instability overturns completely within 300 s or 5 min. The Kelvin–Helmholtz billows, despite this continuous turbulent destruction of shear, endure for more than an order of magnitude longer than the eddy-overturning time scale. The synoptic conditions over Florida do not suggest the existence of any synoptic-scale shear-generating phenomenon. Some local mechanism of the internal cloud dynamics, therefore, must provide this generating mechanism.

During the first half-hour of radar observations, the outflow from the quasi-stationary thunderstorm a few kilometers west of the radar site may have contributed to the generation of shear; however, these storms weakened quickly after dusk. Active lines of thunderstorms oftentimes contain rear-inflow jets that descend beneath the trailing anvil into the storm (Houze et al. 1989), with a front-to-rear flow within the cloud itself. A shear layer must lie between these two air currents; if they occur in sufficient proximity to one another, then shear instability may result. The rear-inflow jet develops internal to the anvil (Houze 1993, p. 385) such that the shear axis will be some distance above the cloud base. We hypothesize that such an anvil internal circulation was responsible for the persistence of the shear instability for the case presented here. The fact that the embedded Kelvin–Helmholtz billows lasted for more than an hour after the demise of the convection requires that an internal circulation within this anvil persisted for the same period.

4. Conclusions

Embedded Kelvin–Helmholtz billows occurred within an anvil over Miami on the evening of 21–22 July 2002. Although previous studies associate large-amplitude shear instability with Kelvin–Helmholtz billow clouds along frontal zones (Chapman and Browning 1997), to our knowledge, these are the first documented large-amplitude, embedded Kelvin–Helmholtz billows inside a tropical anvil. The duration of this phenomenon—more than 3 h—suggests that internal anvil circulations played a role in continuously regenerating the instability, even more than an hour after the demise of all deep convection. The analysis demonstrates that the frequent assumption of an anvil as a well-mixed layer is not always valid. In addition to the main shear axis along which the Kelvin–Helmholtz instability developed, several identifiable weaker shear layers existed in the anvil, evident in the Doppler spread, especially of the aged anvils.

Acknowledgments. Special thanks to Dr. Pavlos Kollias for providing the data, to the Miami Radar Laboratory for collecting the data, and to Robert Carver for several insightful discussions. This work was supported by the National Science Foundation under Grant ATM-0127360.

REFERENCES

Ackerman, T. P., K.-N. Liou, F. P. J. Valero, and L. Pfister, 1988: Heating rates in tropical anvils. *J. Atmos. Sci.,* **45,** 1606–1628.

Babb, D. M., J. Verlinde, and B. A. Albrecht, 1999: Retrieval of cloud microphysical parameters from 94-GHz radar Doppler power spectra. *J. Atmos. Oceanic Technol.,* **16,** 489–503.

Browning, K. A., 1971: Structure of the atmosphere in the vicinity of large-amplitude Kelvin–Helmholtz billows. *Quart. J. Roy. Meteor. Soc.,* **97,** 283–299.

Chapman, D., and K. A. Browning, 1997: Radar observations of wind-shear splitting within evolving atmospheric Kelvin–Helmholtz billows. *Quart. J. Roy. Meteor. Soc.,* **123,** 1433–1439.

Giangrande, S. E., D. M. Babb, and J. Verlinde, 2001: Processing millimeter wave profiler spectra. *J. Atmos. Oceanic Technol.,* **18,** 1577–1583.

Gossard, E. E., and J. H. Richter, 1970: The shape of internal waves of finite amplitude from high-resolution radar sounding of the lower atmosphere. *J. Atmos. Sci.,* **27,** 903–913.

——, D. R. Jensen, and S. H. Richter, 1971: An analytical study of tropospheric structure as seen by high-resolution radar. *J. Atmos. Sci.,* **28,** 794–807.

Houze, R. A., 1993: *Cloud Dynamics.* Academic Press, 573 pp.

——, M. I. Biggerstaff, S. A. Rutledge, and B. F. Smull, 1989: Interpretation of Doppler weather radar displays of midlatitude mesoscale convective systems. *Bull. Amer. Meteor. Soc.,* **70,** 608–619.

Jo, I., B. A. Albrecht, and P. Kollias, 2003: 94-GHz Doppler radar observations of mammatus in tropical anvils during CRYSTAL FACE. Preprints, *31st Int. Conf. on Radar Meteorology,* Seattle, WA, Amer. Meteor. Soc., 197–199.

Kelvin, W. T., 1880: On a disturbing infinity in Lord Rayleigh's solution for waves in a plane vortex stratum. *Nature,* **33,** 45–46.

Kollias, P., B. A. Albrecht, R. Lhermitte, and A. Savtchenko, 2001: Radar observations of updrafts, downdrafts, and turbulence in fair-weather cumuli. *J. Atmos. Sci.,* **58,** 1750–1766.

Lhermitte, R., 1987: A 94-GHz Doppler radar for cloud observations. *J. Atmos. Oceanic Technol.,* **4,** 36–48.

Lilly, D. K., 1988: Cirrus outflow dynamics. *J. Atmos. Sci.,* **45,** 1594–1605.

Martner, B. E., 1995: Doppler radar observations of mammatus. *Mon. Wea. Rev.,* **123,** 3115–3121.

——, and F. M. Ralph, 1993: Breaking Kelvin–Helmholtz waves and cloud-top entrainment revealed by K-band Doppler radar. Preprints, *Ninth Conf. on Atmospheric and Oceanic Waves and Stability,* San Antonio, TX, Amer. Meteor. Soc., 141–144.

Reiss, N. M., and T. J. Corona, 1977: An investigation of a Kelvin–Helmholtz billow cloud. *Bull. Amer. Meteor. Soc.,* **58,** 159–162.

Weckworth, T. A., and R. M. Wakimoto, 1992: The initiation and organization of convection atop a cold-air outflow boundary. *Mon. Wea. Rev.,* **120,** 2169–2187.